

A nonlinear model of an actuator

Pablo V. Negrón–Marrero^a and Eva Campo^b

^aUniversity of Puerto Rico, Department of Mathematics, Humacao, PR 00791;

^bUniversity of Pennsylvania, Laboratory for Research on the Structure of Matter, 3231 Walnut Street, Philadelphia, 19104

ABSTRACT

We present two models based on the theory of nonlinear elasticity of a photo-actuator consisting of a mixture of a polymer matrix with carbon nanotubes. Both models are generalizations of the one proposed by Ahir and Terentjev¹ in which the actuation mechanism is modelled as a contraction of a given carbon nanotube in response to an external stimuli. In the first model, a slight variation is introduced in the projection onto the axis of the pre-strain. This new computation improves the result reported in¹ for carbon nanotube photo-contraction when a 10% pre-strain is applied. In our second model we use a nonlinear constitutive equation to describe the mechanical response of the composite. We show that by a suitable selection of the parameters in the model, consistent with the average constitutive parameters (Young modulus) reported in the literature, we can further improve on the average carbon nanotube contraction for a 10% pre-strain threshold.

Keywords: photo-actuation, composite materials, macro mechanical response, nonlinear elasticity

1. INTRODUCTION

On-going efforts to produce novel materials with improved or augmented functionalities as sensors and actuators frequently focus in smart materials. Smart materials respond to external stimuli in a controlled fashion. Amongst these, stimulus-active polymers (and polymeric composites) are the subject of recent discussion. Indeed, the possibility of microsystem integration and of biocompatibility has opened the door to actuators in Braille displays,¹² artificial muscles,⁴ and drug delivery. In the recent literature, a number of studies have reviewed the current state of the art in shape-memory polymers responsive to a variety of stimuli (heat, light, magnetic and electric fields, and water/solvent media),^{5,9} addressing physical mechanisms inherent to actuation. Historically, thermally-activated shape-memory polymers were first studied and several activation mechanisms have been documented, such as melting transition or in-direction heating amongst others.⁹ Mostly, the physics behind the actuation can be explained by the capacity of the polymer (or polymeric composite), with negligible internal stress in the original state, to store mechanical deformation at lower temperatures. Upon increased temperature, temporary cross-links release mechanical stress, leading to recovery of the original shape.⁵ Electroactive polymers possibly second their thermoactive counterparts in technological advancement. Two activation mechanisms prevail: field actuation and ionic diffusion.⁴ In field-activated systems, a Coulomb electrostatic field induces conformational changes by dipole aligning and Ionic electroactive polymers involve ion diffusion upon field activation; where the macroscopic motion of charged species is responsible for actuation.

Lastly, a novel actuation mechanism has been reported for polymer-carbon nanotube composites.¹ In this scheme, irradiation of a source with distribution centered at 675 nm promotes actuation stresses of up to 100 kPa which confers a change in natural length of up to 10% within ~ 0.5 min.² These are promising characteristics for microelectronic applications, where fast, reversible actuation is preferred to, for example, thermally-induced processes. On that note, it is worth mentioning that although the temperature during actuation augments by $\sim 15^\circ\text{C}$, thermal saturation occurs after a few minutes of irradiation, therefore dismissing heat as trigger. In addition, the photomechanical response of MWCNTs embedded in a silicon rubber PDMS matrix is a new effect-not associated to a magnifying mechanism due to the presence of MWCNTs, as the pristine elastomer shows

Further author information:

P.V.N–M.: E-mail: pnm@mate.uprh.edu

E.C.: E-mail: campoem@seas.upenn.edu

a minimal response to the same irradiation source due to heating. Although both expansion and contraction-actuation modes are possible (arguably, depending on the degree of alignment due to pre-applied strains), the magnitude of the stroke depends solely on the matrix, suggesting the possibility of photoactuation as a universal phenomenon in polymer-MWCNT composites.

This paper is motivated by the work of Ahir and Terentjev¹ in which they describe a simple model based on the theory of (linear) elasticity, for the mechanism of photo-actuation of a composite of a polymer matrix with nanotubes inclusions. The basic assumption in their model is that a given carbon nanotube contracts (via an incompressible nanotube deformation) by a ratio Δ under the influence of an external energy source. The nanotube is assumed to be cylindrical with the contraction along the principal axis of the cylinder. The (linear) projection of this deformation onto the principal axis of pre-strain of the specimen is then averaged over all possible directions yielding an average nanotube actuation deformation along the pre-strain axis. This average is then included in the equation for the (macro) stress-strain relation (Hooke's law type) yielding a simple model that predicts the observed change in mechanical behavior in the composite due to the external energy source.

We call the *critical value of pre-strain* to the value of the (macro) strain at which the stress-strain curves, with and without an external energy source, intersect. In other words, it is the pre-strain under which the composite does not show macroscopic actuation. Larger pre-strains would induce an average contraction upon illumination and smaller pre-strains would induce an average expansion, but at the specific critical value of pre-strain, the composite remains macroscopically inactive upon irradiation. In laboratory experiments with various polymer-nanotube composites at different concentrations of nanotubes, it has been observed that this critical pre-strain value is approximately 10%. The model in¹ predicts that for a critical pre-strain value of 10%, the average contraction per nanotube should be around 20%, i.e. $\Delta \approx 0.8$. However, laboratory data reveals that the actual critical pre-strain value is achieved with only a 1-2% average contraction per nanotube ($\Delta \approx 0.98$). With a slight change in the model in¹ in the way the projection of the nanotube deformation onto the principal axis of strain is computed, we can improve on their results to a 10-13% nanotube deformation for a 10% critical pre-strain value.

Experimental description of the Ahir-Terentjev photo-actuation system

Contrary to the other actuation modes, the physical mechanism behind photomechanical actuation remains unknown, with some indicators leaning towards the importance of nanotube alignment in the matrix.^{1,2} In^{1,2} the authors first reported photomechanical effects in PDMS-MWCNT composites¹ and later in a variety of polymeric systems.² Specifics on composites preparation can be found in the original reports and we will focus on the PDMS composite preparation here. Briefly, PDMS silicon elastomer and hydrosilane curing agents were purchased from Dow Corning and the resulting polymer network was absent of filler particles. The MWCNTs were purchased from Nanostructured and Amorphous Materials, Inc. (Houston, TX). The MWCNTs presented a verifiable 95% purity, with core and outer diameters of 5-10 and 60-100 nm respectively, and lengths between 5 and 15 μm .

The composite was fabricated by shear mixing of MWCNTs and silicon elastomer for at least 24 hours. The cross-linker was then added and further mixed for another 30s, and left in vacuum for 5 min to degas. The mixture was placed in a centrifuge reactor at 5000 rpm and 80°C for 14 min to expedite cross-linking and produce films of uniform thickness. Upon centrifugation, the partially-cross-linked film was uniaxially strained to infer a mechanically-aligned distribution of MWCNTs in the matrix and the cross-linking was finalized under the applied stress in an oven at 70°C for an additional 24 h. Several composites with MWCNT concentrations of 0, 0.02, 0.3, 0.5, 1, 2, 3, 4, and 7 wt% were prepared in this fashion.

It is worth to emphasize here the use of shear mixing in MWCNTs in an effort to not alter the external chemical structure of CNTs. In this work, the authors were careful not to modify the surface chemistry of the MWCNTs, in an attempt to minimize formation of additional sp³-hybridized defects.

A light source with peak emission at 675 nm was the promoter of the actuation, with an estimated power density delivered to the sample of $\sim 1.5\text{mW}/\text{cm}^2$. Pristine PDMS films showed absorption of $\sim 3\%$ and 0.3wt% PDMS-MWCNTs absorbed in excess of 97% across a range of wavelengths.

Each sample was clamped under pre-applied strains ranging between 2 and 40%. This set up was assembled in a specially designed thermally-insulated rig, where vertical deformations could be measured with a μm precision and the exerted force upon actuation was measured by sensitive dynamometers. Thermocouples attached to the front and back of the film, registered thermal kinetics saturated within two minutes of light irradiation. Kinetics of the actuation itself maximized within 0.5 m of irradiation. This argument, combined with the observed order of magnitude difference for thermally-induced deformation, suggests that the actuation described here is not of thermal nature.

Following this experimental set up, responses of a 1wt% PDMS composite to irradiation under applied pre-strain is shown in Figure 7 in.² Notably, for low applied pre-strains (below 10%), the composite expands upon irradiation. However, applied pre-strains above 10% yield contraction. This phenomenon seems to be common to composites of varying MWCNT concentration; all switching actuation direction around 10% pre-applied strain. A tentative explanation for this phenomenon takes into account the realignment of MWCNTs in the matrix for the different pre-applied strains.

2. THE MATHEMATICAL MODELS

We consider a composite formed of a polymer matrix with nanotubes inclusions. We assume perfect bonding between the two phases and that the composite is uniform and isotropic. Also, we assume each nanotube to be a cylindrical (slender) structure, the principal axis been the axis of the cylinder. We will study the effects of non-linearity on the forecast average contraction per nanotube Δ dictated by a 10% critical pre-strain value. The non-linearity study will be performed in two stages; first, considering a semi-linear model and introducing a fully non linear model in a later stage. Adoption of this stepped approach, will facilitate the assessment of the incorporation of non-linearities in photoactuation. Indeed, the semi-linear model still considers an incompressible deformation but will make use of a non-linear stretch of the deformation along a principal axis (unlike in¹). In the non-linear approach, a non-linear stress-strain constitutive equation along with the hypothesis of compressibility will be used.

2.1 The semi-linear model

Let (θ, ψ) be angles in spherical coordinates with respect to a cartesian coordinate system $\{\mathbf{i}, \mathbf{j}, \mathbf{k}\}$, where θ is the angle with respect to \mathbf{k} and ψ is the angle with respect to \mathbf{i} in the \mathbf{ij} plane. Define:

$$\mathbf{e}_1(\theta, \psi) = \cos \theta \cos \psi \mathbf{i} + \cos \theta \sin \psi \mathbf{j} - \sin \theta \mathbf{k}, \quad (1a)$$

$$\mathbf{e}_2(\theta, \psi) = -\sin \psi \mathbf{i} + \cos \psi \mathbf{j}, \quad (1b)$$

$$\mathbf{e}_3(\theta, \psi) = \sin \theta \cos \psi \mathbf{i} + \sin \theta \sin \psi \mathbf{j} + \cos \theta \mathbf{k}. \quad (1c)$$

If the composite is subject to a (macro) deformation λ along the z axis and assuming the specimen undergoes an incompressible deformation, the corresponding deformation gradient is given by:

$$\mathbf{F}_m = \frac{1}{\sqrt{\lambda}} (\mathbf{i} \otimes \mathbf{i} + \mathbf{j} \otimes \mathbf{j}) + \lambda \mathbf{k} \otimes \mathbf{k}. \quad (2)$$

If a given nanotube has spherical angles (Θ, ψ) before this macro deformation, then after the deformation \mathbf{F}_m the angle ψ remains the same, but Θ changes to θ where:

$$\begin{aligned} \cos \theta &= \frac{\mathbf{k} \cdot \mathbf{C}_m \cdot \mathbf{e}_3(\Theta, \psi)}{\sqrt{\mathbf{k} \cdot \mathbf{C}_m \cdot \mathbf{k}} \sqrt{\mathbf{e}_3(\Theta, \psi) \cdot \mathbf{C}_m \cdot \mathbf{e}_3(\Theta, \psi)}} \\ &= \frac{\lambda^{3/2} \cos \Theta}{[\sin^2 \Theta + \lambda^3 \cos^2 \Theta]^{1/2}}, \end{aligned} \quad (3)$$

and $\mathbf{C}_m = \mathbf{F}_m^t \mathbf{F}_m$. (Note that $\mathbf{e}_3(\Theta, \psi)$ points along the principal axis of the nanotube cylinder before the macro deformation.) Using this relation one can easily get that:

$$\tan \Theta = \lambda^{3/2} \tan \theta, \quad \sin \Theta d\Theta = \frac{\lambda^3 \sin \theta}{[\cos^2 \theta + \lambda^3 \sin^2 \theta]^{3/2}} d\theta.$$

We assume that the effect of photo actuation is given by a contraction by a factor of Δ along the principal axis of a nanotube cylinder. In the pre-strained composite, that is, after the deformation \mathbf{F}_m , the deformation gradient corresponding to an *incompressible* deformation of the nanotube is given by:

$$\mathbf{F}_a = \frac{1}{\sqrt{\Delta}} (\mathbf{e}_1(\theta, \psi) \otimes \mathbf{e}_1(\theta, \psi) + \mathbf{e}_2(\theta, \psi) \otimes \mathbf{e}_2(\theta, \psi)) + \Delta \mathbf{e}_3(\theta, \psi) \otimes \mathbf{e}_3(\theta, \psi). \quad (4)$$

The principal stretch along the \mathbf{k} axis (henceforth called the z axis) corresponding to this deformation is given after simplification by:

$$\lambda_z(\theta, \Delta) = \|\mathbf{F}_a \cdot \mathbf{k}\| = \left[\Delta^2 \cos^2 \theta + \frac{1}{\Delta} \sin^2 \theta \right]^{1/2}. \quad (5)$$

Remark: In¹ the authors used the linearization of this stretch about $\mathbf{F}_a = \mathbf{I}$ (which is when $\Delta = 1$). This linearized stretch along the z axis is given by:

$$\varepsilon_z(\theta, \Delta) = \Delta \cos^2 \theta + \frac{1}{\sqrt{\Delta}} \sin^2 \theta. \quad (6)$$

In our first modification of their model, we use (5) which is geometrically more accurate than (6).

With these formulas we can compute the *average stretch upon actuation* by averaging over all possible nanotube orientations:

$$\hat{\lambda}_z(\Delta, \lambda) = \frac{1}{4\pi} \int_0^{2\pi} \int_0^\pi \lambda_z(\Theta, \Delta) \sin \Theta \, d\Theta d\psi = \int_0^\pi \lambda_z(\theta, \Delta) P_\lambda(\theta) d\theta, \quad (7)$$

where

$$P_\lambda(\theta) = \frac{\lambda^3 \sin \theta}{2 [\cos^2 \theta + \lambda^3 \sin^2 \theta]^{3/2}}. \quad (8)$$

One can check that $\int_0^\pi P_\lambda(\theta) d\theta = 1$, and since $P_\lambda(\theta) \geq 0$, we can interpret $P_\lambda(\theta) d\theta$ as the probability of finding nanotubes making angles with the z axis in the range $[\theta, \theta + d\theta]$, after the composite is subjected to the macro deformation λ along the z axis.

The stress-strain response of the composite along the z axis is given by the linear relation (Hooke's law):

$$S = Y(\lambda - 1), \quad (9)$$

where the *Young modulus* Y is an average of the mechanical properties of the polymer-nanotube composite. The corresponding stress due to photo-actuation will be modeled with:

$$S_{act} = Y(\hat{\lambda}_z(\Delta, \lambda) - 1). \quad (10)$$

Note that (9) is linear in λ but (10) is not due to the nonlinear dependence of P_λ on λ (cf. (8)). The net macro stress along the z axis is given by:

$$S_{net} = S - S_{act} = Y(\lambda - \hat{\lambda}_z(\Delta, \lambda)). \quad (11)$$

Note that S and S_{net} cross or intersect precisely for those values of (Δ, λ) for which:

$$\hat{\lambda}_z(\Delta, \lambda) = 1. \quad (12)$$

Note that this condition depends only on the photo-actuation parameter Δ and the macro strain λ , and not on the Young modulus Y ! (This might be a limitation of the semi-linear model.) Experimentally it has been determined that this crossing occurs for $\Delta \approx 0.98$ and $\lambda \approx 1.1$, pretty much independent of the composite.² In the terminology of the introduction, we have that the critical pre-strain value is approximately 10%.

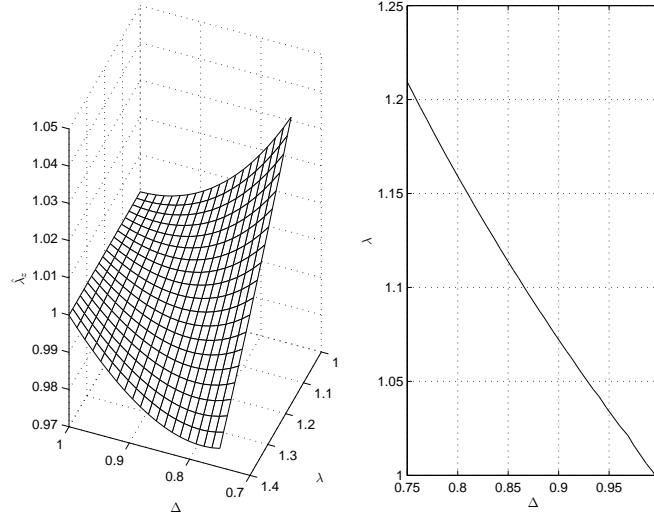


Figure 1. (Left) The surface $\hat{\lambda}_z(\Delta, \lambda)$ as a function of (Δ, λ) for $0.75 \leq \Delta \leq 1.0$ and $1 \leq \lambda \leq 1.4$. (Right) Level curve $\hat{\lambda}_z(\Delta, \lambda) = 1$.

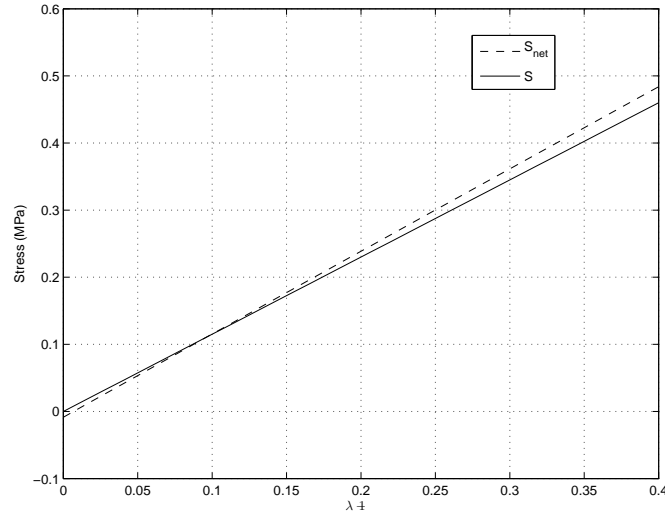


Figure 2. Graphs of S and S_{net} as predicted by the model for an average nanotube contraction factor of $\Delta = 0.87$.

For the numerical simulations we used a value of $Y = 1.15$ MPa as reported in¹ for the average Young modulus of the 1 wt% PDMS composite they used in their experiments. We first show in the left hand side of Figure 1 a surface for the values of $\hat{\lambda}_z(\Delta, \lambda)$ as a function of (Δ, λ) for $0.75 \leq \Delta \leq 1.0$ and $1 \leq \lambda \leq 1.4$. On the right hand side of the same figure we show the level curve of this surface at height one. This corresponds to the solution set of equation (12) for $0.75 \leq \Delta \leq 1.0$ and $1 \leq \lambda \leq 1.4$. From this plot we can read that the model predicts a crossing of S and S_{net} at $\lambda = 1.1$ for a value of $\Delta = 0.87$ approximately. For this value of Δ , we show in Figure 2 the graphs of S and S_{net} as predicted by the model. These results are in agreement with the corresponding ones reported in¹. In Figure 3 we show the graph of the effect of photo-actuation as measured by the difference $S_{net} - S$. The dotted line in this plot joining the initial and final points, is just for reference to emphasize the nonlinear behavior of photo-actuation.

The value of $\Delta = 0.87$ predicted by the model is smaller than the one observed experimentally of 0.98, but better than the one predicted by the model in¹ using (6) instead of (5).

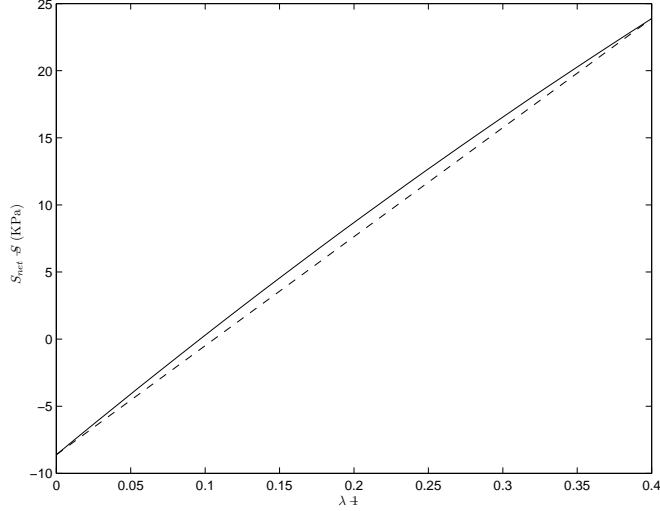


Figure 3. Effect of photo-actuation as measured by the difference $S_{net} - S$.

2.2 A nonlinear model

We discuss now a model which uses a nonlinear stress-strain constitutive equation for the response of the composite. The idea is that with a more general model of mechanical behavior, we may be able to capture more details of the physics of the actuation process.

As before, we assume that the composite is subject to a (macro) deformation of λ along the z axis. Instead of the incompressibility assumption we had before, we consider now a compressible deformation with deformation gradient given by:

$$\mathbf{F}_m = \mu(\lambda) (\mathbf{i} \otimes \mathbf{i} + \mathbf{j} \otimes \mathbf{j}) + \lambda \mathbf{k} \otimes \mathbf{k}, \quad (13)$$

where $\mu(\lambda)$ is a function to be determined by the boundary conditions. A calculation similar to the one before shows that if a given nanotube has spherical angles (Θ, ψ) before this macro deformation, then after the deformation \mathbf{F}_m the angle ψ remains the same, but Θ changes to θ where:

$$\cos \theta = \frac{\lambda \cos \Theta}{[\mu^2(\lambda) \sin^2 \Theta + \lambda^2 \cos^2 \Theta]^{1/2}}, \quad (14)$$

and that:

$$\tan \Theta = \frac{\lambda}{\mu(\lambda)} \tan \theta, \quad \sin \Theta d\Theta = \frac{\lambda^2 \mu(\lambda) \sin \theta}{[\mu^2(\lambda) \cos^2 \theta + \lambda^2 \sin^2 \theta]^{3/2}} d\theta.$$

We keep the same assumptions on a given nanotube deformation due to photo-actuation so that formulas (4) and (5) still hold. Using the formulas above, we have that the average stretch upon actuation is given now by:

$$\hat{\lambda}_z(\Delta, \mu(\lambda), \lambda) = \int_0^\pi \lambda_z(\theta, \Delta) Q(\theta, \mu(\lambda), \lambda) d\theta, \quad (15)$$

where

$$Q(\theta, \mu(\lambda), \lambda) = \frac{\lambda^2 \mu(\lambda) \sin \theta}{2 [\mu^2(\lambda) \cos^2 \theta + \lambda^2 \sin^2 \theta]^{3/2}}. \quad (16)$$

As before Q can be interpreted as a probability distribution for the angular distribution of nanotubes in the deformed macro specimen.

We now describe the mechanical response of the composite. The proposed model is based on the theory of nonlinear elasticity as described, e.g., in.³ Let $W : \text{Lin}^+ \rightarrow \mathbb{R}$ be the *stored energy function* of the composite

(assumed to be homogenous) where $\text{Lin}^+ = \{\mathbf{F} \in M^{3 \times 3} : \det \mathbf{F} > 0\}$ and $M^{3 \times 3}$ denotes the set of real 3×3 matrices. The first Piola–Kirchhoff and Cauchy stress tensors are respectively given by:

$$\mathbf{S}(\mathbf{F}) = \frac{d}{d\mathbf{F}}W(\mathbf{F}), \quad \boldsymbol{\sigma}(\mathbf{F}) = (\det \mathbf{F})^{-1}\mathbf{S}(\mathbf{F})\mathbf{F}^t. \quad (17)$$

The material of the composite is *isotropic* if there exists a function $\hat{W} : (0, \infty)^3 \rightarrow \mathbb{R}$ such that*:

$$W(\mathbf{F}) = \hat{W} \left(\frac{1}{2} \mathbf{F} \cdot \mathbf{F}, \frac{1}{4} \mathbf{F}\mathbf{F}^t \cdot \mathbf{F}\mathbf{F}^t, \det \mathbf{F} \right). \quad (18)$$

We now have that:¹¹

$$\mathbf{S}(\mathbf{F}) = \hat{W}_{,1}\mathbf{F} + \hat{W}_{,2}\mathbf{F}\mathbf{F}^t\mathbf{F} + (\det \mathbf{F})\hat{W}_{,3}\mathbf{F}^{-t}. \quad (19)$$

For the function \hat{W} we use the following (Hadamard–Green type) expression:

$$\hat{W}(v_1, v_2, v_3) = av_1 + b(v_1^2 - v_2) + cv_3^\gamma + dv_3^{-\delta}, \quad (20)$$

where $a, d, \delta > 0$, and $b, c, \gamma \geq 0$. Combining (17), (19), and (20) we get that for the deformation (13):

$$\boldsymbol{\sigma}(\mathbf{F}_m) = \text{diag}(\sigma_{11}(\mu, \lambda), \sigma_{22}(\mu, \lambda), \sigma_{33}(\mu, \lambda)), \quad (21)$$

where $\sigma_{11}(\mu, \lambda) = \sigma_{22}(\mu, \lambda)$ and

$$\sigma_{11}(\mu, \lambda) = (\mu^2\lambda)^{-1} \left([a + b(\mu^2 + \lambda^2)] \mu^2 + c\gamma(\mu^2\lambda)^\gamma - d\delta(\mu^2\lambda)^{-\delta} \right) \quad (22a)$$

$$\sigma_{33}(\mu, \lambda) = (\mu^2\lambda)^{-1} \left((a + 2b\mu^2)\lambda^2 + c\gamma(\mu^2\lambda)^\gamma - d\delta(\mu^2\lambda)^{-\delta} \right). \quad (22b)$$

We require that the reference configuration be stress free, that is $\mathbf{S}(\mathbf{I}) = \mathbf{0}$, which implies that:

$$a + 2b + c\gamma - d\delta = 0. \quad (23)$$

Also if we require that the linearization of (19) about $\mathbf{F} = \mathbf{I}$ coincides with the linear theory of Section 2.1, then we get the additional condition on the parameters in (20):

$$Y = 3(a + b). \quad (24)$$

We take as boundary conditions that $\sigma_{11} = \sigma_{22} = 0$ which leads to:

$$[a + b(\mu^2 + \lambda^2)] \mu^2 + c\gamma(\mu^2\lambda)^\gamma - d\delta(\mu^2\lambda)^{-\delta} = 0. \quad (25)$$

This equation determines μ as a function of λ . If we write

$$t_z(\lambda) = \sigma_{33}(\mu(\lambda), \lambda),$$

then equations (9), (10), and (11) are given now by:

$$S = t_z(\lambda), \quad (26a)$$

$$S_{act} = t_z(\hat{\lambda}_z(\Delta, \mu(\lambda), \lambda)), \quad (26b)$$

$$S_{net} = S - S_{act}. \quad (26c)$$

Note that S and S_{net} cross or intersect precisely for those values of (Δ, λ) for which:

$$\hat{\lambda}_z(\Delta, \mu(\lambda), \lambda) = 1. \quad (27)$$

*The first argument in \hat{W} measures local deformations of fibers, the second one measures local surface deformations, while the third argument (the determinant) measures local volume changes.

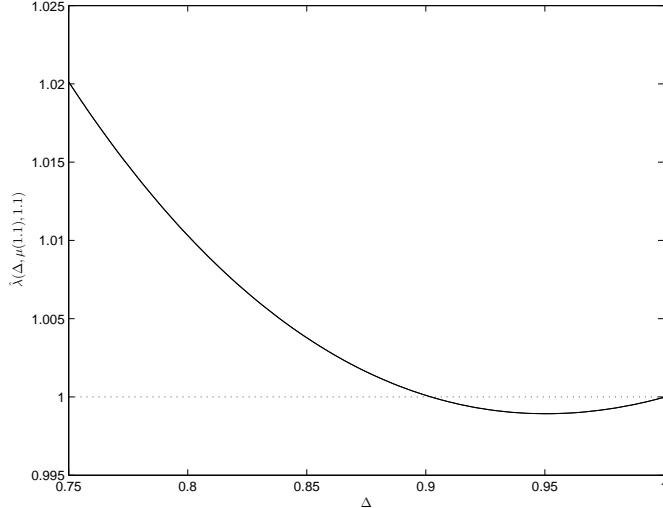


Figure 4. Graph of $\hat{\lambda}_z(\Delta, \mu(1.1), 1.1)$ for the parameters (28) with a, d chosen to satisfy (23) and (24), and $Y = 1.15$.

Note that now, contrary to the model of Section 2.1, this equation depends on all the mechanical parameters in (20) through $\mu(\lambda)$ which is given as the solution of (25).

For the simulations we used the following values for the parameters in (20):

$$b = 0.01, \quad c = 0.1, \quad \delta = 0.1, \quad \gamma = 0.1, \quad (28)$$

and a, d are chosen to satisfy (23) and (24), with $Y = 1.15$ MPa. In Figure 4 we show a sketch of $\hat{\lambda}_z(\Delta, \mu(\lambda), \lambda)$ for the fixed value of $\lambda = 1.1$ corresponding to a pre-strain of 10% for the composite. We see from this figure that the crossing of S and S_{net} (cf. (27)) would occur at a 10% pre-strain for a $\Delta = 0.9$ approximately. (The values in (28) were chosen after some trial and error, to maximize the value of Δ for this crossing.) Figure 5 shows the corresponding graphs in this case for S and S_{net} . We note a difference in the size of the stresses (smaller in this model) corresponding to those in Figure 2, of 20–25% for less than 20% pre-strain, up to roughly 40% for 40% pre-strain. This could be accounted for by the compressibility assumption that makes the material of the composite somewhat “easier” to deform. Thus the compressible model does not reproduce that well the magnitude of the stresses but predicts a better average nanotube contraction factor ($\Delta \approx 0.90$).

In² Young modulus for nanocomposites were reported in the range of 0.5 up to 1.5 MPa approximately depending on the wt% concentration, with errors in the order of ± 0.1 . In Figure 6 we show the same graphs as above but for[†] $Y = 1.25$. In this case we have better agreement with the corresponding values in Figure 2 for pre-strains less than 20%, with the differences again increasing up to roughly 30% for 40% pre-strain. Thus some of the differences in the values of the stresses as predicted by the nonlinear compressible model might be attributed to experimental errors present in the reported Young modulus.

3. CONCLUSIONS AND COMMENTS

In this work, we have reproduced in some detail the model proposed by Ahir and Terentjev^{1,2} to explain photoactuation of nanocomposites. Change of direction in photoactuation at particular pre-strains offers an opportunity to correlate macroscopic deformations in the composite with nanoscopic deformations in the fillers. In this scheme, a linear model predicts large values of nanotube contractions which have not fully been verified experimentally. The predicted nanotube contraction can be lowered by optimizing calculations either in the projection or by computing non linear deformations in a compressible solid. With all, major questions still remain at the atomic level regarding the nature of the polymer–nanotube interface.^{6,7,13} In addition, specifics

[†]For $Y = 1.25$, the value of Δ for a crossing of S and S_{net} at a 10% pre-strain, is again 0.9 approximately.

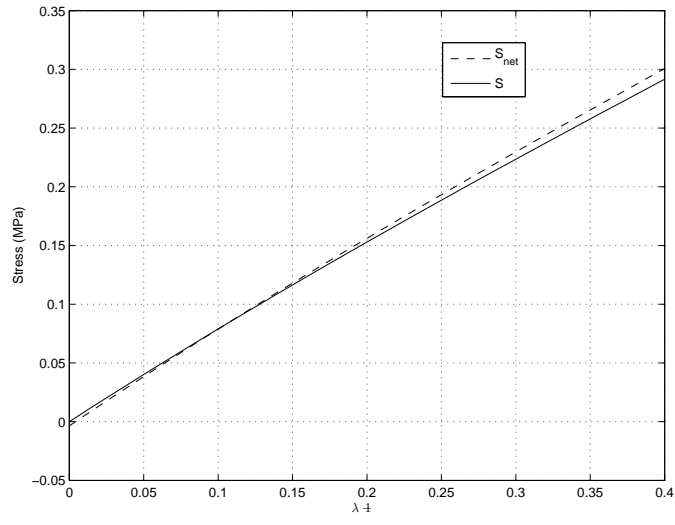


Figure 5. Graphs of (26a) and (26c) for the compressible model with $Y = 1.15$.

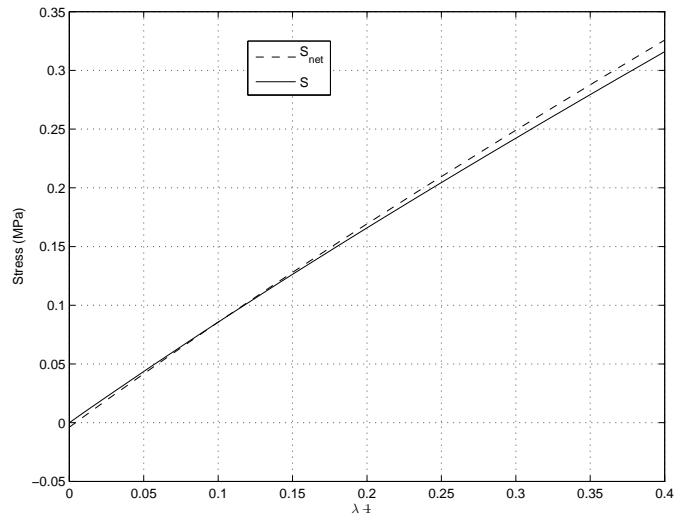


Figure 6. Graphs of (26a) and (26c) for the compressible model with $Y = 1.25$.

about the mechanisms for nanotube contraction, bending, or torsion in the matrix need further study. For instance, it is known that the radial response of a CNT is very different from the axial response.^{10,14} This radial response might be important when computing the nanotube average stretch upon actuation in (7) or (15). A full treatment based on the theory of composite materials⁸ might be useful to account for these additional effects.

ACKNOWLEDGMENTS

This research was sponsored in part (Negrón–Marrero) by the Partnership for Research and Education in Materials (PREM) program of the University of Puerto Rico at Humacao. We gratefully acknowledge partial funding (Campo) from the EU FP7 under contract NMP 228916.

REFERENCES

- [1] Ahir, S. V and Terentjev, E. M., “Photomechanical actuation in polymernanotube composites,” *Nature Materials*, Vol. 4, 491–495, June (2005).
- [2] Ahir, S. V., Squires, A. M., Tajbakhsh, A. R., and Terentjev, E. M., “Infrared actuation in aligned polymer-nanotube composites,” *Physical Review*, B 73, 085420, (2006).
- [3] Antman, S. S., [*Nonlinear Problems of Elasticity*], Springer Verlag, New York, (2000).
- [4] Bar-Cohen, Y. and Zhang, Q., “Electroactive Polymer Actuators and Sensors,” *MRS Bulletin*, Vol. 33, 3, 173-177, March (2008).
- [5] Behl, M., Razzaq, M.Y., and Lendlein, A., “Multifunctional Shape-Memory Polymers,” *Adv. Mater.*, 22, 3388-3410, (2010).
- [6] Desai, A.V. and Haque, M.A., “Mechanics of the interface for carbon nanotube–polymer composites”, *Thin-Walled Structures* 43, 1787–1803, (2005).
- [7] Giulianini, M. et. al., “Evidence of multiwall carbon nanotube deformation caused by poly(3-hexylthiophene) adhesion”, *Journal of Physical Chemistry C*, 115, 6324–6330, (2011).
- [8] Hill, R., “On constitutive macro-variables for heterogeneous solids at finite strain,” *Proceedings Royal Society of London*, A. 326, 131-147, (1972).
- [9] Meng, H. and Hu, J., “A Brief Review of Stimulus-active Polymers Responsive to Thermal, Light, Magnetic, Electric, and Water/Solvent Stimuli,” *Journal of Intelligent Material Systems and Structures*, Vol. 21, 9, 859-885, June (2010).
- [10] Palaci, I., Fedrigo, S., Brune, H., Klinke, C., Chen, M., and Riedo, E., “Radial elasticity of multiwalled carbon nanotubes”, *Physical Review Letters*, 94, 175502 (2005).
- [11] Simpson, H. C. and Spector, S. J., “On barrelling instabilities in finite elasticity,” *Journal of Elasticity*, 14:103–125, (1984).
- [12] Smella, E., “Conjugated Polymer Actuators”, *MRS Bulletin*, Vol. 33, 197–204, March (2008).
- [13] Wong, M., Paramsothy, M., Xu, X.J., Ren, Y., Li, S., and Liao, K., “Physical interactions at carbon nanotube–polymer interface”, *Polymer* 44, 7757–7764, (2003).
- [14] Yang, Y.H. and Li, W.Z., “Radial elasticity of single-walled carbon nanotube measured by atomic force microscopy”, *Applied Physics Letters* 98, 041901, (2011).